ISIJ International, Vol. 31 (1991), No. 5, pp. 440-448

Kinetic Analysis of Coke Gasification Based on Non-crystal/Crystal Ratio of Carbon

Yoshiaki KASHIWAYA and Kuniyoshi ISHII

Department of Metallurgical Engineering, Faculty of Engineering, Hokkaido University, Kita-ku, Kita-13, Nishi-8, Sapporo, Hokkaido, 060 Japan.

(Received on November 16, 1990; accepted in the final form on January 25, 1991)

Gasification of metallurgical coke was studied at 1 000, 1 200 and 1 400°C with Ar – CO – CO_2 mixtures. Reaction of coke in blast furnace is dominant from 1 000°C. And at the same time, growth of graphite crystal in coke begins around the temperature.

In present paper, two types of carbon structure were classified by means of X-ray diffraction. One is crystallite that contributes to X-ray diffraction, the other is noncrystalline carbon that contributes to background intensity alone. In this study, reaction model that the two kinds of carbon have different reactivity and react simultaneously and independently, was developed and kinetic analysis was performed. The following results were obtained.

(1) *Lc* is linear function of temperature and there is no influence of reaction.

(2) *La* is linear function of temperature in Ar atmosphere. But in existence of reaction, the size of *La* becomes to be smaller. From this result, it was considered that the gasification reaction proceeds such as mode of decreasing *La*. Reaction mechanism combining to characteristic of crystallographic structure is proposed.

KEY WORDS: metallurgical coke; gasification; kinetic analysis; crystalline size of carbon; reaction mechanism; X-ray diffraction.

1. Introduction

There have been many investigations about coke behaviors in blast furnace (BF), due to the significant influences of strength and reactivity on the BF operations. A lot of studies such as kinetics,[1,2] effect of physical properties on the reactivity[3-6] and change of reactivity in blast furnace,[3,7] have been reported. However, the rate constants obtained in kinetic analysis could not generally applied to different sample, since the wide variety of coke properties arise from the property of coking coal and history of coke making.

In blast furnace, carbon solution loss reaction (gasification) of coke is dominant from about 900°C, and growth of graphite crystal (crystallite) in coke begins to occur simultaneously from that temperature. It is generally thought that the reactivity of carbonaceous material decreases with degree of graphitization, conversely, it becomes more active as close to non-crystal carbon.[8] Even if the effect of ash and other impurities on reactivity are excepted, the gasification reaction is much more complex so that there are many crystals having various graphitization degree in different proportions. Moreover, graphite crystals grow up with temperature in blast furnace. It can be thought that the large scattering of reactivity of coke originates from the different distribution of graphitization degree of carbon crystals.

Hitherto, the reactivity of coke and graphitization process of carbon crystal have been separately discussed. The multiplicity of crystal of carbon has not been considered in kinetic analysis but treated as homogeneous material. In this study, using X-ray diffraction method, the effects of temperature and gasification reaction on the size of crystallite in coke were investigated. The microscopic gasification mechanism of coke was discussed based on those results. Moreover, reaction model combined with characteristics of crystallographic structure was proposed, in which two kinds of crystal (crystallite having low reaction rate and non-crystal carbon having high reaction rate) coexisted in coke and proportion of each kind of crystal was varied with temperature. Using this model, kinetic analysis was performed.

2. Gasification Model of Coke

Practical coke consists of many kinds of carbon crystal having various graphitization degree, as the details will be mentioned below. In this study, however, the kinds of carbon crystal were classified into two types for simplification of kinetic analysis. One is graphite crystal (crystallite) that contributes to X-ray diffraction and the other is non-crystal carbon (that is distinguished from amorphous or free carbon here and constructed with a few six-membered ring. Also a few six-membered rings do not contribute the X-ray diffraction) that contributes the background intensity alone. Simple model of gasification and crystallization of coke was illustrated in Fig. 1. Gasification of both the crystallite having low reaction rate

and non-crystal carbon having high reaction rate occurs simultaneously (①, ②). At the same time, graphitization of non-crystal carbon independently proceeds (③). As a result, the non-crystal carbon is incorporated into crystallite depending on reaction temperature. Here, the rate of graphitization (③) is so fast and non-crystal carbon changes to crystallite at a given proportion immediately after the reaction temperature increases (>900°C).

2.1. *Growth of Crystallite and Gasification Mechanism*

X-ray diffraction of sample has been performed to investigate the effect of temperature and gasification on the size of crystallite. Fig. 2(a) shows the schematic diagram of graphite crystal and the unit cell. The size of crystallite can be represented by the spread of carbon net plane (*La*) and the thickness of carbon net layer (*Lc*).[8] Fig. 2(b) illustrates the concept of crystallite with *La* and *Lc*. The values of *La* and *Lc* can be estimated by SCHERRER's equation[3,9] as follows:

$$L_{hkl} = A\lambda/(B\cos\theta) \quad \text{.....(1)}$$

where, A: a constant given by reflection plane (L_{002}; $A=0.9$, L_{10}; $A=1.84$)

λ: the wavelength of X-ray (Å) employed

B: half-value width (rad)

θ: the reflection angle of peak.

Usually, in the case of low graphitized carbon, since the two reflections of (100) and (101) plane superimpose and become into one peak, they are represented as (10). The conditions of sample preparation such as particle size, packing pressure to sample and flatness of surface of packing sample affect the X-ray diffraction pattern, the measurement of X-ray diffraction has been carried out under unified conditions. In this study, the milling time of sample by vibration mill, which has important effect on crystallite size, was fixed to 10 s for 1 g coke sample. The packing method of sample to X-ray sample holder was also unified to obtain the same back ground level. Then good reproducibility has been attained.

Fig. 3 shows the X-ray diffraction patterns of metallurgical coke before and after heat treatment at 1 450°C in Ar atmosphere for 1 h. The largest constituent in ash of coke is SiO_2 and next one is Al_2O_3 (Table 1). The SiO_2 in coke takes a form of Quartz (ASTM 33-1162)[3] before heat treatment.

Peak width of (002) reflection is broad before heat treatment and it indicates that the *Lc* is small. After the heat treatment, the peak becomes sharper according to the enlargement of *Lc*. The peak of (10) reflection corresponding to *La* becomes also sharper. It represents that the crystallite has grown as temperature increase.

Fig. 4 shows X-ray diffraction patterns of coke after gasification at various temperatures, when the degree of gasification is from 10 to 30 % and the details of experiment will be mentioned below. At 1 000°C, the peak of (002) was still broad, however,

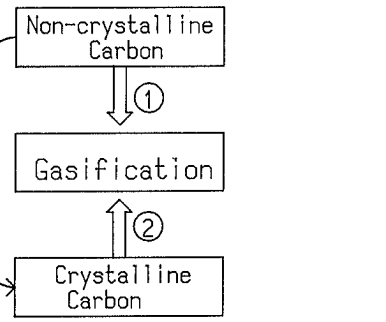

Fig. 1. Processes of gasification and crystallization of carbon.

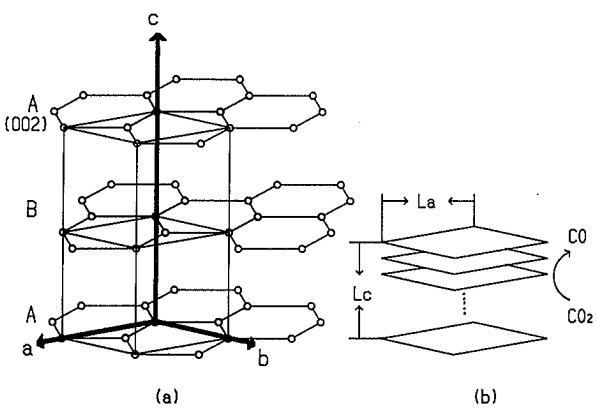

(a) Unit cell of graphite crystal
(b) Relationship between crystallite and *La*, *Lc*

Fig. 2. Schematic diagrams of graphite crystallite.

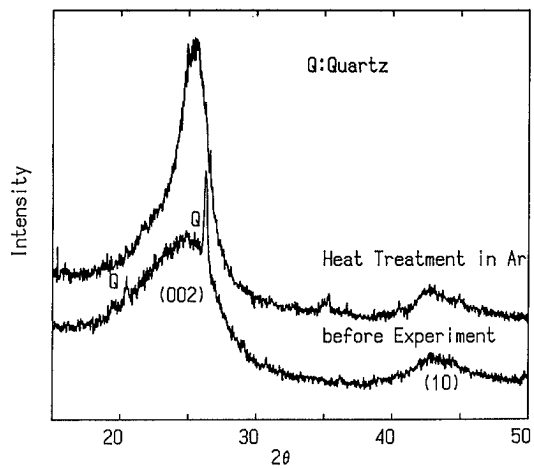

Fig. 3. X-ray diffraction patterns of heat treated and non-treated metallurgical coke.

Table 1. Chemical composition and physical properties of metallurgical coke.

Chemical composition (wt%)								Apparent density (g/cm³)	Mean diameter (mm)	Void fraction (—)
T.Fe	SiO_2	Al_2O_3	CaO	MgO	S	Fixed C	Volatile matter			
1.1	6.0	3.3	0.3	0.2	0.7	87.5	0.9	1.05	1.59	0.495

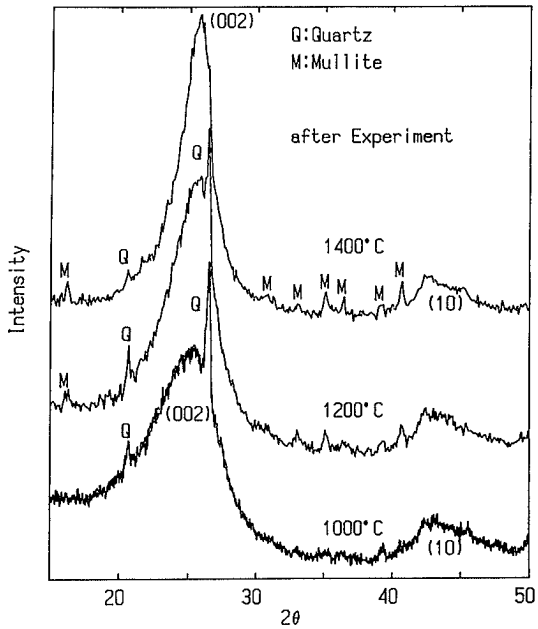

Fig. 4. X-ray diffraction patterns of metallurgical coke at various reaction temperatures.

according to increasing temperature, the peak became sharper and it revealed the growth of crystallite (*Lc*). It was clearly confirmed after the gasification at 1 400°C that Quartz in ash has reacted with Al_2O_3 and Mullite (ASTM 15-776) was formed.

The values of *Lc* and *La* are estimated from the half-value width of these peaks using Eq. (1) and shown in Figs. 5 and 6, respectively.

Fig. 5 shows the *Lc* of various temperatures. *Lc* (●) of coke undergone gasification increased linearly as temperature increased. In addition, *Lc* had the same tendency after heat treatment in Ar atmosphere (■: 60 min, □: 5 min). So it was thought that the *Lc* was determined by reaction temperature and independent to atmosphere and gasification reaction. On the other hand, *La* was smaller after gasification (Fig. 6) than that heated in Ar atmosphere. These facts indicate that the gasification reaction proceeds preferentially on the specified crystallographic plane, the rate of gasification is slow in the (002) plane (plane of carbon net) and fast in the plane perpendicular to (002) plane.

It could be considered that the first elementary reaction in gasification is adsorption of CO_2, and that the site where CO_2 molecule is able to adsorb in a crystallite, is dangling bond rather than defects in the plane of carbon net. Further, the dangling bond exists in the periphery of carbon net plane (or in the side of crystallite, Fig. 2(b)).

2.2. *Method of Kinetic Analysis*

2.2.1. Rate Equation Considering Graphitization of Carbon

Several kinds of Langmuir–Hinshelwood (L–H) type rate equation have been presented[11] for analyzing the rate of coke gasification. In this study, the successive elementary reactions are proposed according to the results mentioned above. It is assumed

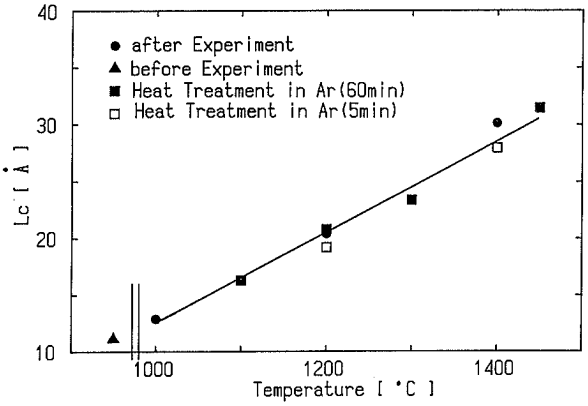

Fig. 5. Relationship between *Lc* and temperature.

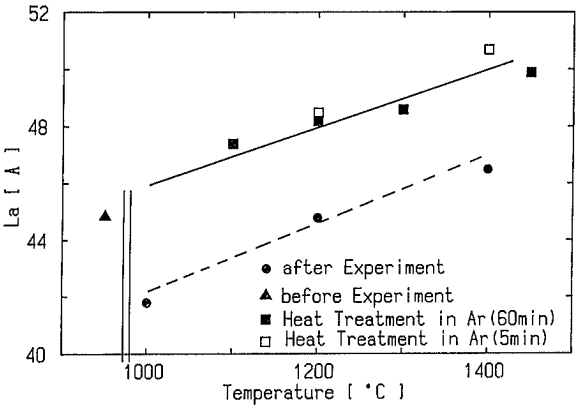

Fig. 6. Relationship between *La* and temperature.

that the carbon atoms having dangling bond become adsorption site. A CO_2 molecule adsorbs to this carbon atom as first elementary reaction. Prior to considering the subsequent elementary reactions, interatomic distance and geometric configuration for the both of CO_2 and graphite should be considered for determining the formation of CO_2 molecule adsorbed. That is whether two oxygen atoms in CO_2 adsorb at the same time or only one oxygen atom.

(I) C and O in CO_2 are in a line and the distance is 1.16 Å, or distance from O to O atom is 2.32 Å.[14]

(II) Distance of nearest neighbor atom in carbon net plane is 1.42 Å and distance of second nearest neighbor atom is 2.46 Å. Interlayer distance of graphite is 3.35–3.44 Å.[8]

From (I) and (II), it could be considered that the adsorbing oxygen is one oxygen in CO_2 not the both oxygens at the same time. Then following reaction mechanism could be thought as illustrated in Fig. 7 schematically.

① CO_2 adsorbs on the carbon (C_f) having dangling bond (Eq. (2)).

② CO_2 adsorbed is dissociated into O and CO. Then CO gas is liberated (Eq. (3)).

③ O adsorbed on C_f becomes CO gas (Eq. (4)).

④ Adsorption of CO gas on C_f and desorption from C_f occur simultaneously and independent to those of CO_2 molecule (Eq. (2)').

Following equations of elementary reaction are given for successive reactions of (2) to (4) and (2)'.

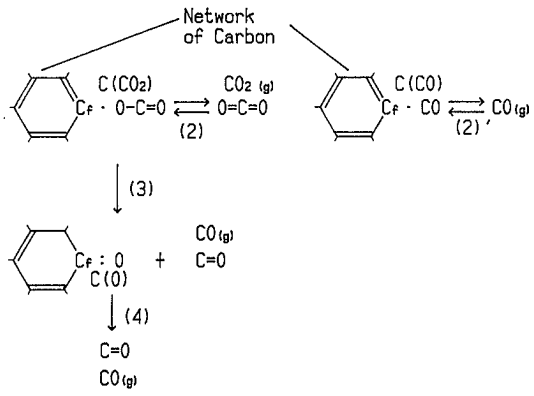

Fig. 7. Schematic diagram of elementary reactions related with graphite crystalline characteristic.

$$C_f + CO_{2(g)} \underset{i_2}{\overset{i_1}{\rightleftharpoons}} C(CO_2) \quad \text{.....(2)}$$

$$C(CO_2) \xrightarrow{i_3} C(O) + CO_{(g)} \quad \text{.....(3)}$$

$$C(O) \xrightarrow{i_4} CO_{(g)} \quad \text{.....(4)}$$

$$C_f + CO_{(g)} \underset{i_6}{\overset{i_5}{\rightleftharpoons}} C(CO) \quad \text{.....(2)'}$$

where, C_f: carbon atom having dangling bond and corresponds to adsorption site

C(O), C(CO), $C(CO_2)$: O, CO and CO_2 adsorbed on the dangling bond carbon atom, respectively.

Sum of adsorption site per unit volume (C_T, mol/cm^3) is divided by density of crystallite (ρ_0) and represented as dimensionless number ($S_T = 12\ C_T/(\rho_0)$). This dimensionless concentration of adsorption site, S_T implies the number of adsorption site per a carbon atom.

$$S_T = S_\theta + S_f \quad \text{.....(5)}$$

where, $S_\theta (= S_{CO_2} + S_{CO} + S_O)$: ratio of adsorption site occupied by atom or molecule

S_f: the empty site.

Assuming the reaction (4) is the rate controlling step, the following relationships are obtained on the basis of steady state.

$$i_1 P_{CO_2} S_f = i_2 S_{CO_2} + i_3 S_{CO_2} \quad \text{.....(6)}$$

$$i_3 S_{CO_2} = i_4 S_O \quad \text{.....(7)}$$

$$i_5 P_{CO} S_f = i_6 S_{CO} \quad \text{.....(8)}$$

The overall reaction rate k is

$$k = i_4 S_O \quad \text{.....(9)}$$

Using Eqs. (6) to (8), Eq. (9) is transformed to Eq. (9)'.

$$k = i_1 i_3 / (i_2 + i_3) P_{CO_2} S_f$$
$$= k_1 S_T P_{CO_2} / (1 + k_2 P_{CO} + k_3 P_{CO_2}) \quad \text{.....(9)'}$$

where, $k_1 = i_1 i_3 / (i_2 + i_3)$

$k_2 = i_5 / i_6$

$k_3 = (i_1 i_3 + i_1 i_4) / (i_2 i_4 + i_3 i_4)$

P_{CO}, P_{CO_2}: partial pressure (atm) of CO and CO_2, respectively.

Eq. (9)' can be taken as a modified L–H type rate equation, in which the fractional overall adsorption site is newly introduced. It was assumed that the reaction mechanism was basically the same as distinct crystallites having different graphitization degree. The number of adsorption site per a carbon atom, that the sites exist at the periphery of carbon net, decrease as the dimension of carbon net (La) increase. This results in the decrease of carbon reactivity. When carbon crystals in coke are classified roughly into two types according to graphitization degree, crystal and non-crystal, the number of adsorption site per a carbon atom (S_T) of non-crystal carbon are larger than that of crystal carbon and reactivity of non-crystal carbon is larger.

Since the number of adsorption site is unknown for the both types of carbon. In this study, to estimate the reaction rate for the two kinds of carbon separately, resultant, $k_1 \cdot S_T$ are taken as apparent rate constant. Then Eq. (9)' is separated to Eqs. (10) and (11) for crystal and non-crystal carbon, respectively:

$$k_c = k_{1,c} \cdot P_{CO_2} / (1 + k_2 P_{CO} + k_3 P_{CO_2}) \quad \text{.....(10)}$$

$$k_a = k_{1,a} \cdot P_{CO_2} / (1 + k_2 P_{CO} + k_3 P_{CO_2}) \quad \text{.....(11)}$$

where, subscripts c, a: crystal, and non-crystal carbon, respectively.

2.2.2. Relationship between La and Reactivity

It is assumed in this study that the adsorption site is the carbon having dangling bond which exists in the periphery of carbon net. The number of adsorption site (carbon having dangling bond) per a carbon atom S_T varies according to the size of La. La is not constant and decreases with the extent of gasification (Fig. 6). Therefore, strictly speaking, reactivity of carbon also changes during gasification and is different with each crystals which have different graphitization degree. From this reason, the relationship between the size of La and the number of adsorption site has been considered as mentioned below.

Number of carbon which exists in periphery of carbon net is varied with morphology of carbon net. In order to estimate the number of carbon having dangling bond at first, the configuration of carbon net composed of a lot of six-membered ring must be postulated. So it was assumed that the growth of basal plane of graphite crystal in coke is isotropic and the carbon net develops in the manner of maintaining a similar figure to basal plane (a–b plane) of unit cell of graphite. When number of six-membered ring which exits in one side of carbon net parallelogram are varied to 1, 2, 3, 4, . . . , n, the whole number of six-membered ring are given as 1, 4, 9, 16, . . . , n^2 in a carbon net. For example, in the case of $n=3$, the graphite a–b plane is illustrated in Fig. 8, where the carbon having dangling bond is represented as solid circle (●). Total number of carbon atom C_T and the number of carbon having dangling bond F_T are

$$C_T = 2n(n+2) \quad \text{.....(12)}$$

$$F_T = 4n+2 \quad \text{.....(13)}$$

respectively. Then the ratio of adsorption site S_T is

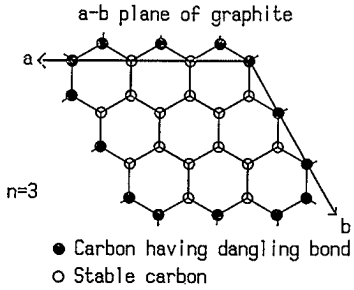

Fig. 8. Model of carbon network having dangling bond ($n=3$). It is postulated that graphite crystal equiaxially develops on a–b plane of unit cell.

$$S_T = (4n+2)/(2n(n+2)) \quad \text{.....(14)}$$

The relationship between S_T and n^2 (whole number of six-membered ring) is shown in Fig. 9. In the present experiment, La increases from 45 Å (1 000°C) to 50 Å (1 400°C) during heating in Ar (Fig. 6), the change of n can be estimated from 18 (1 000°C) to 20 (1 400°C) using La obtained and lattice constant ($a=$ 2.46 Å), and total number of six–membered ring per a carbon net is from 324 to 400. Then fraction of dangling bonded site scarcely varies from 0.103 to 0.093 and can be taken as to be constant. Also, even though the degree of gasification is as large as 70 % and La decreases to about 40 Å, S_T merely increases to about 0.11. Because rate controlling step might be change to mass transfer of gaseous constituent in product layer (ash layer) and the fixed bed employed also alters in packing characteristics, when the degree of gasification exceeds 30 %, kinetic analysis in the present study is restricted up to only 30 % of gasification.

On the other hand, since non-crystal carbon is thought to be built up by several six-membered rings,[8] the fraction of adsorption site ($S_{T,a}$) is 5 to 9 times as large as crystallite (Fig. 9). In practice, the value of observed $k_{1,a}$ are 5 to 20 times larger as it will be shown in Fig. 13 and prediction from the model mentioned above is in good agreement with observation. From these reasons, it is thought that the fraction of adsorption site ($S_{T,c}$) of crystallite is constant in the temperature range of this experiment and therefore the rate constant $k_{1,c}(=k_1 \cdot S_{T,c})$ can be dealt with as a function of temperature for the coke used.

2.2.3. Kinetic Analysis

Kinetic analysis has been performed on the basis of chemical reaction control. The rate of gasification reaction per unit volume of bed, R_G(mol/s/cm³-bed) is defined as to be proportional to unreacted carbon (Eq. (15)).

$$R_G \equiv -dC/dt = kC = k(1-X)C_0 \quad \text{.....(15)}$$

$$X = (W_0 - W)/W_0 \quad \text{.....(16)}$$

where, C: concentration (mol/cm³-bed)
W: weight
X: fractional gasification
0: the initial time ($t=0$).

Eqs. (15) and (16) are independently applied for the both rate of reaction of crystal and non-crystal carbon.

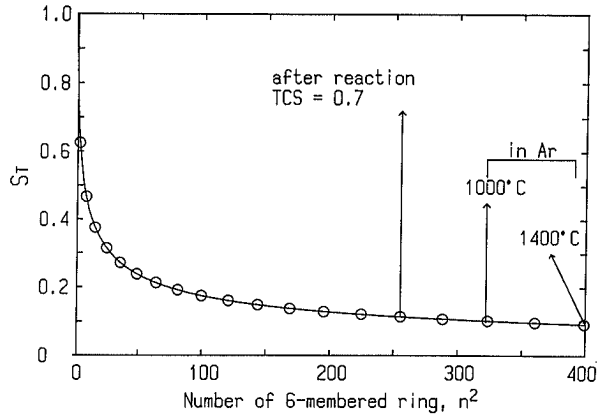

Fig. 9. Relationship between the number of dangling bond per carbon atom (S_T) and six-membered ring (n^2).

It is necessary to evaluate the initial weight of crystal and non-crystal carbon ($W_{c,0}$, $W_{a,0}$) in advance for proceeding the calculation, because the reactions of crystal and non-crystal carbon proceed independently. Since Lc and La (Figs. 5 and 6) increase linearly with increasing temperature (1 000–1 400°C) under no reaction, empirical formula of Lc and La are obtained from Figs. 5 and 6 (Lc(Å)$=-29+0.042 \cdot T$(°C), La(Å)$=34+0.011 \cdot T$(°C)). Then the initial weight of crystal carbon can be estimated from Eq. (17) and that of non-crystal carbon is obtained from Eq. (18).

$$W_{c,0} = n_c \cdot V_c \cdot \rho_0 \quad \text{.....(17)}$$

$$W_{a,0} = W_0 - W_{c,0} \quad \text{.....(18)}$$

$$n_c = W_0/V_{c,1400} \cdot \rho_0 \quad \text{.....(19)}$$

where, $V_c(=Lc \cdot La^2 \cdot (\sqrt{3}/2) \times 10^{-24}$ [cm³]): the mean volume of a crystallite
$\rho_0(=2.21$(g/cm³)[8]): the density of crystallite.

n_c is the whole number of crystallite contained in coke sample and determined by Eq. (19) from the viewpoint of nucleation of crystallite. The number of nuclei for crystal growth are constant above 1 000°C, that is, the nucleation is completed before coke goes up to 1 000°C and only the size of crystallite increases with temperature, in addition, all non-crystal carbon are incorporated into crystal carbon at 1 400°C. Temperature variations of $W_{a,0}$ and $W_{c,0}$ are shown in Fig. 10 as the fractional weight ($N_c = W_{c,0}/W_0$, $N_a = W_{a,0}/W_0$) corresponding to Lc and La obtained from Figs. 5 and 6, respectively.

As the degree of gasification is varied between bottom and top of the bed due to concentration distribution of reaction gas, the observed rate of reaction should be analyzed by the method for a packed bed. Assuming one-dimensional distribution of gas concentration along flow axis, mass balances for gas components, CO and CO_2 can be obtained in a thin volume element of packed bed.

$$u(\partial P_{CO}/\partial z) + \varepsilon(\partial P_{CO}/\partial t) = 2 \cdot R_G \cdot RT \quad \text{.....(20)}$$

$$u(\partial P_{CO_2}/\partial z) + \varepsilon(\partial P_{CO_2}/\partial t) = -R_G \cdot RT \quad \text{.....(21)}$$

On the other hand, mass balance of carbon in coke is

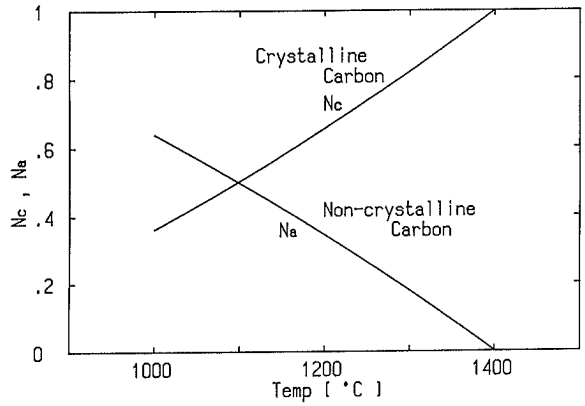

Fig. 10. Variation of N_a, N_c with temperature.

Eq. (22).

$$\partial X_c/\partial t = \partial(X_c+X_a)/\partial t = R_{G,c}\cdot 12/C_{c,0}+R_{G,a}\cdot 12/C_{a,0} \quad \text{.....(22)}$$

where, P: partial pressure of gas components (atm)
R: gas constant
$R_G(=R_{G,a}+R_{G,c}$: mol/s/cm^3-bed): rate of gasification reaction
T: absolute temperature
u: superficial velocity of gas (cm/s)
z: distance along gas flow (cm)
ε: void fraction of bed (—).

The kinetic analysis has been performed by solving the equations (Eqs. (15), (16) and (20) to (22)) simultaneously for crystal and non-crystal carbon, respectively. Then the partial differential equations were transformed to ordinary differential equations by using the characteristic curve method.

3. Experimental

Fig. 11 shows a schematic diagram of experimental apparatus. Ar, CO and CO_2 were adjusted by mass flow controller (MFC) so as to make a given composition. These gases were mixed through the mixer and introduced to reaction chamber. Gas analysis was carried out by means of infra-red gas analyzer about CO and CO_2. The analyzers was calibrated by using standard gas which was precisely arranged to near composition with exhausted gas. Reaction furnace was vertical type electric furnace having SiC heater and reaction tube made of mullite (35 mm, I.D.×600 mm, L). Crucible was an alumina tube (20 mm I.D.) and alumina sieve was fixed at bottom to form the reactor with 40 mm depth. When 5 g of coke sample was put in the crucible, about 30 mm height of packing column was formed.

Metallurgical coke crushed into 9–16 mesh and was used for experiment without heat treatment. Chemical composition and physical properties of metallurgical coke are given in Table 1.

Total flowrate of reaction gas was 2 000 cm^3/min (STP) (superficial velocity of gas was about 11 cm/s) and in a few experiment the flowrate was increased for evaluating the characteristics of fixed bed. Experiments were carried out at temperatures of 1 000, 1 200 and 1 400°C, simulating the coke gasification from chemical reserve zone to lower part of cohesive zone in blast furnace. Concentration range of CO in reaction gas was 0–40 vol% and CO_2 was 2–30 vol% diluted with Ar. The ratio of CO/CO_2 was appropriately changed. Pressure was fixed and 101.3 kPa (1 atm).

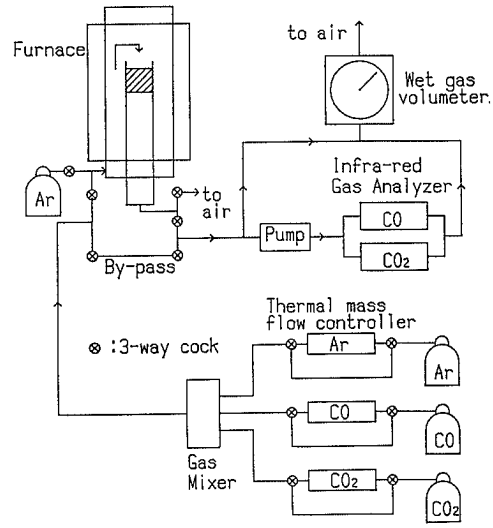

Fig. 11. Schematic diagram of experimental apparatus.

4. Results and Discussion

4.1. *Effects of Reaction Conditions on Gasification*

Relationship between observed rate of gasification (RCS [1/s]) and concentration of reaction gas CO and CO_2 are plotted in Fig. 12 at temperatures of 1 000, 1 200 and 1 400°C. The results can be summarized as follows:

(a) Effects of CO_2

(i) In low CO_2 regime (<10 %), reaction rate increased linearly with concentration.

(ii) In high CO_2 regime, the gradient of the rate curve became small with concentration. It shows the presence of inhibition effect of CO_2 on gasification rate.

(iii) The inhibition effect of CO_2 was remarkable at low temperature (1 000°C) and it became smaller as the temperature increased.

(b) Effects of CO

(i) There was a inhibition effect of CO gas on gasification reaction. It was remarkable in lower concentration range.

(ii) The inhibition effect of CO was almost disappear at high temperature (1 400°C).

4.2. *Determination of Rate Constants*

At first, it was examined whether the reaction in this experiment was controlled by mass transfer[12] or not. The rate of gas film mass transfer calculated from Ranz's equation[13] has been larger by a factor of about 100 than the observed gasification rate. This evaluation is not so accurate that the calculation is not based on the mixed control. However, it is enough to demonstrate that the resistance of mass

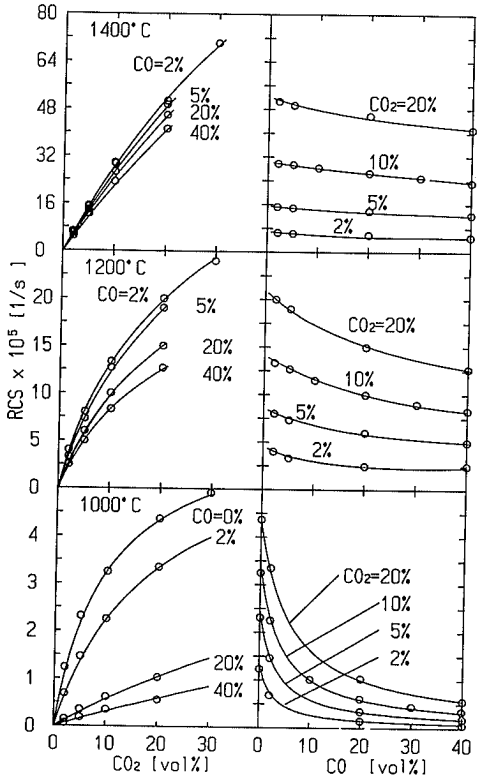

Fig. 12. Variation of RCS with experimental conditions.

transfer in gas film is negligibly small. Moreover, that effect was confirmed to be small by experiments[12] in which total flowrate of reaction gas increased to 3 000 and 3 500 cm³/min (STP). In this case, the observed rate of reaction increased as the gas flowrate increased. However, it was ascertained by calculation as fixed bed mentioned above that the tendency could be explained sufficiently by the modifying of distribution of gas concentration in packed column. However, the most important problem in mass transfer is gas diffusion in pore of coke particle than gas film mass transfer. Then the rate of pore diffusion of gas (1 000°C, $P_{CO_2}=0.2$, $P_{CO}=0$) has been calculated using effective diffusion coefficient from Kobayashi and Ohmori.[15] The calculated value is larger than the observation by a factor of about 120. It indicates that the contribution of gas diffusion in particle can be also neglected.

In order to determine the rate parameters based on the chemical reaction control, Eqs. (15), (16) and (20) to (22) were solved simultaneously. It is important to estimate the adequate initial value so as to avoid a risk of getting meaningless values and to conduct the effective calculation of parameter fitting by using the trial and error method.

In this study, based on the following two assumptions, the approximate values have been estimated.

① C_c and C_a are constant ($C_c=C_{c,0}$, $C_a=C_{a,0}$).

② No distribution of gas concentration in packed column. (The observed mean value of gas compositions between inlet and outlet gas of bed were used.)

At the quite initial period ($\fallingdotseq$60 s) of observed curve of gasification rate, assumption ① will be valid and Eq. (15) is modified as follows:

$$-dC_c/dt \fallingdotseq k_c \cdot C_{c,0} \quad \text{.....(23)}$$

$$-dC_a/dt \fallingdotseq k_a \cdot C_{a,0} \quad \text{.....(24)}$$

Therefore, observed gasification rate (RCS) is expressed by adding Eqs. (23) and (24).

$$-dC/dt \fallingdotseq k_c \cdot C_{c,0} + k_a \cdot C_{a,0}$$
$$= (k_{1,c} \cdot C_{c,0} + k_{1,a} \cdot C_{a,0}) P_{CO_2} / (1 + k_2 P_{CO} + k_3 P_{CO_2}) \quad \text{.....(25)}$$

$$\text{RCS} = -(dC/dt) \cdot 12 \cdot V_B / W_0$$
$$= k_0 \cdot P_{CO_2} / (1 + k_2 P_{CO} + k_3 P_{CO_2}) \quad \text{.....(26)}$$

where, $k_0 = (k_{1,c} \cdot C_{c,0} + k_{1,a} \cdot C_{a,0}) \cdot 12 V_B / W_0$ .....(27)

V_B: bed volume.

Using observed value of gasification rate (RCS), the rate constants in Eq. (26) were determined as starting value for calculation. The reciprocal of RCS was proportional to $1/P_{CO_2}$ and P_{CO}/P_{CO_2} in which P_{CO} and P_{CO_2} were dealt with constant based on the assumption ②. Then k_0, k_2 and k_3 were obtained by the linear multiple regression analysis and $k_{1,c}$, $k_{1,a}$ could be roughly evaluated from Eq. (27) using a critical value at 1 400°C ($C_a=0$, $k_0=k_{1,c}$). The intrinsic values of $k_{1,c}$, $k_{1,a}$, k_2 and k_3 were obtained by fitting the calculated rate curve to the observed one. In this case, the calculation converged with 20 s of time interval and 30 divisions of height of packed bed.

The rate constants are expressed as temperature dependency.

$$k_{1,c} = \exp(9.49 - 24\,200/T) \quad \text{.....(28-a)}$$

$$k_{1,a} = \exp(4.19 - 13\,400/T) \quad \text{.....(28-b)}$$

$$k_2 = \exp(-17.7 + 27\,700/T) \quad \text{.....(28-c)}$$

$$k_3 = \exp(-1.59 + 5\,680/T) \quad \text{.....(28-d)}$$

The obtained rate constants ($k_{1,c}$, $k_{1,a}$ ($s^{-1} \cdot atm^{-1}$), k_2 (atm^{-1}), k_3 (atm^{-1}), solid circles (●)) are also compared with the results of Kobayashi and Ohmori[1] (broken line) and Aderibigbe and Szekely[2] (dash-dotted line) in Fig. 13. The $k_{1,a}$ is larger than others and $k_{1,c}$ is smaller in the present study. If the reactivity of coke is established by only crystal/non-crystal ratio of carbon, the rate constants of the present study will be useful to evaluate the reactivity of different kind of coke. Moreover, it is considered that rate data for preheated at high temperature, though almost other experiments have been carried out with preheated sample, could not be applied to evaluate the coke behavior in blast furnace, because temperature history of sample has a major influence on crystal/non-crystal ratio. k_2 and k_3 have a negative temperature dependency, contrary to k_1, that reflects the experimental results (Fig. 12), which the inhibition effect on gasification rate decreases with temperature.

TCS and RCS calculated by using the rate constants obtained are compared with observed one in Figs. 14 to 16 for each temperature.

Fig. 14 shows the results of gasification with 20%CO_2–0%CO gas mixture at 1 000°C. All kinds of line correspond to calculation. It is found that the results of calculation were in good agreement with

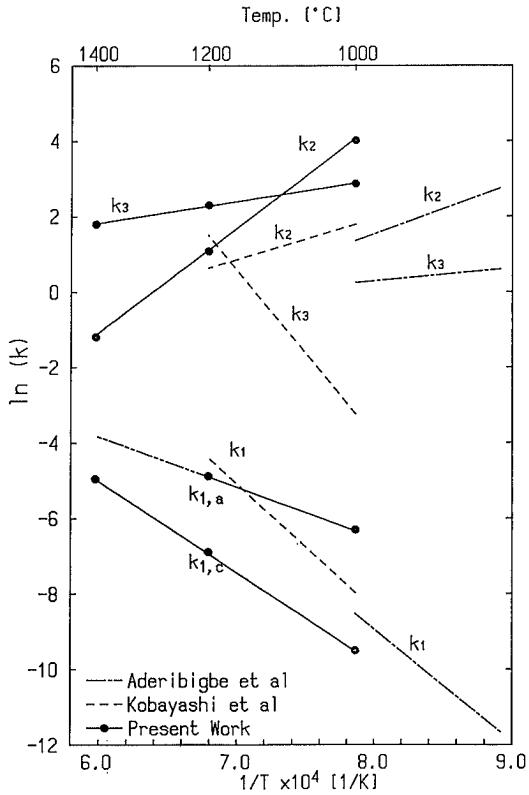

Fig. 13. Arrhenius plot of rate constants.

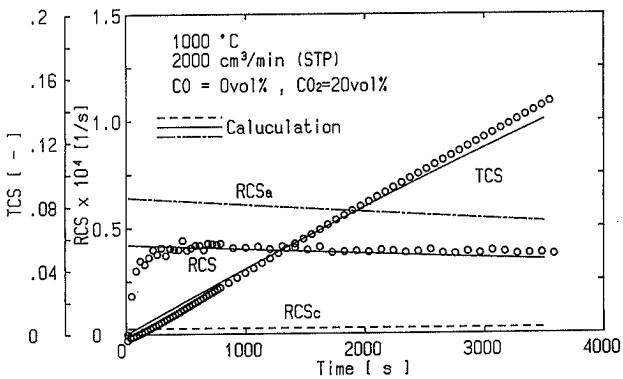

Fig. 14. Comparison between calculated results and observed data (1 000°C).

observed one.

Fig. 15 shows the results of gasification with 20%CO_2–2%CO gas mixture at 1 200°C. In this case, the rate of gasification is relatively high, so that the difference between the observed and calculated data increased, as the degree of gasification exceeds 30 % at 2 000 s. There are some reasons for this phenomenon,

a) ash layer begins to appear at the upper part of bed (inlet side of gas), and consequently,
b) the height of packed bed becomes short.

At 1 000°C, the contribution of crystallite (RCS_c) to overall rate of reaction (RCS) is small. However, the proportion of RCS_c to overall rate at 1 200°C extensively increases compared with that of 1 000°C and RCS_c is mostly kept at constant value within the experiment time. On the other hand, the rate of reaction of non-crystal carbon (RCS_a) decreased monotonously with time. Nevertheless it is appeared at 1 200°C yet that gasification mainly proceeds at non-crystal carbon.

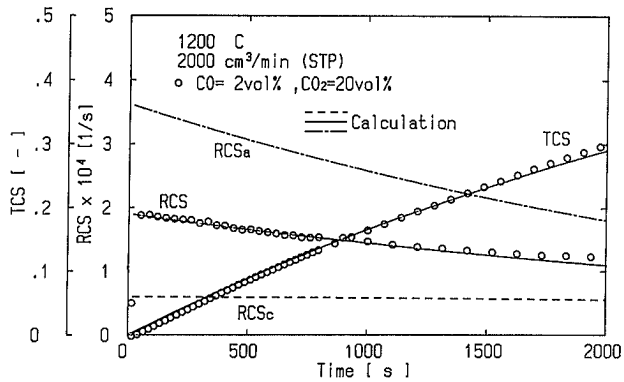

Fig. 15. Comparison between calculated results and observed data (1 200°C).

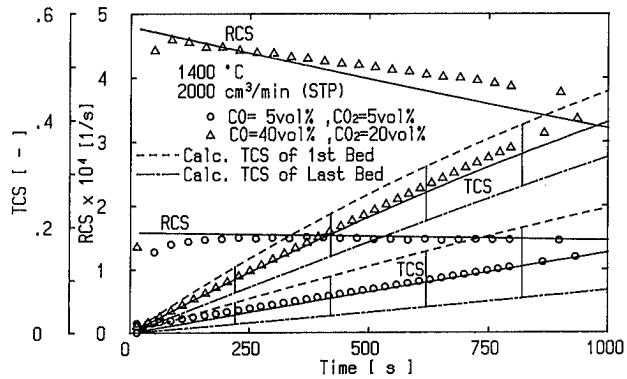

Fig. 16. Comparison between calculated results and observed data ($RCS=RCS_c$ at 1 400°C).

The comparison of calculation with observation at 1 400°C is shown in Fig. 16, where two sets of data are illustrated with the different composition of reaction gas. One is high CO_2 content to generate the higher rate of gasification (△), the other is low CO_2 content (○). All results of calculation are represented by some kinds of line. Not only the apparent degree of gasification (averaged degree of overall beds: solid line) but also the degrees of gasification at the first-sectioned bed (broken line) and the last-sectioned bed (30th bed: dash-dotted line) are concurrently plotted. These show the time-dependent variation of distribution of gasification degree (TCS) in packed column.

5. Conclusions

The crystal of carbon in coke were roughly classified into two types by means of X-ray diffraction. One was crystallite that contributed to X-ray diffraction, the other was non-crystal carbon that contributed only to background intensity. Reaction model that the two kinds of carbon have different reactivity and react with gas simultaneously and independently, was developed and the kinetic analysis was performed. The conclusions obtained are as follows:

From the result of X-ray diffraction

(1) *Lc* linearly increased with temperature independently on the atmosphere and gasification reaction.

(2) *La* increased with temperature in Ar atmosphere.

However, *La* decreased after gasification. From these results, the mechanism of gasification has been newly proposed: gasification proceeds at preferential crystallographic direction and only *La* decreases.

From the results of gasification experiment

(3) In gasification of coke, the rate of gasification was not proportional to the concentration of CO_2 and in the case of high CO_2 content, there was a inhibition effect of CO_2 inversely.

(4) There was a inhibition effect of CO on gasification. It was remarkable in low CO concentration regime and the effect was almost disappear at high temperature.

(5) Considering the two kinds of carbon having different reactivity, the rate constants were obtained with modified Langmuir–Hinshelwood type rate equation.

REFERENCES

1) S. Kobayashi and Y. Ohmori: *Tetsu-to-Hagané*, **63** (1977), 1081.
2) D. A. Aderibigbe and J. Szekely: *Ironmaking Steelmaking*, **8** (1981), 11.
3) J. V. Dubrawski and W. W. Gill: *Ironmaking Steelmaking*, **11** (1984), 7.
4) Y. Suminami and M. Ogawa: *Coke Circular*, **26** (1977), 262.
5) H. Fujita, M. Hijiriyama and K. Nishida: *Coke Circular*, **29** (1980), 218.
6) T. Ishihara, Y. Yoshino and K. Tsuchibashi: *Coke Circular*, **26** (1977), 249.
7) K. Kojima, N. Nishi, T. Yamaguchi and H. Nakama: *Tetsu-to-Hagané*, **62** (1976), 570.
8) K. Kobayashi: The Introduction of Carbon Materials, Soc. Carbon Mater., Tokyo, (1972), 12.
9) H. P. Klug and L. E. Alexander: X-ray Diffraction Procedures for Polycrystalline and Amorphous Materials, John Wiley & Sons, New York, (1954).
10) B. P. Richards: *J. Appl. Crystallogr.*, **70** (1972), 84.
11) P. L. Walker, Jr., F. Rusinko, Jr. and L. G. Austin: *Advan. Catalysis*, **XI** (1959), 133.
12) S. Kondo, K. Ishii, Y. Kashiwaya, K. Yamashita and S. Nakaya: Report of 54th Comm. (Ironmaking), Japan Soc. Promotion of Sci. (JSPS), Rep. No. 54-1851 (Feb. 1988).
13) W. E. Ranz: *Chem. Eng. Prog.*, **48** (1952), 247.
14) Y. Kitano, M. Ichikawa, T. Cho, S. Inoue and K. Asada: Chemistry of Carbon Dioxide, Kyoritu Shuppan, Tokyo, (1976).
15) S. Kobayashi and Y. Ohmori: *Tetsu-to-Hagané*, **64** (1978), 187.